

Fracture Dynamics by Quenching. I. Crack Patterns

Yasuhide MORI, Kunihiko KANEKO[†] and Miki WADATI

*Department of Physics, Faculty of Science, University of Tokyo,
Hongo 7-3-1, Bunkyo-ku, Tokyo 113*

*[†]Department of Pure and Applied Sciences, College of Arts and Sciences,
University of Tokyo, Komaba, Meguro-ku, Tokyo 153*

(Received December 17, 1990)

A dynamical lattice model is presented to simulate fracture of brittle materials caused by quenching. With this model, relations between fracture patterns and temperature difference in quenching are investigated. It is found that as the temperature difference increases, a tree-like (a few branched) pattern suddenly changes into a net-like (many branched) pattern.

§1. Introduction

It is almost sixty years ago that M. Hirata studied fractures in various materials and observed a variety of patterns of cracks.¹⁻³⁾ For instance, cracks of glass show various beautiful patterns depending on the condition of blow or quenching. Figure 1 adapted from ref. 2 shows a typical example of a fracture pattern when a small spot of a glass plate is heated in high temperature and is left. In this case it has been discovered that one crack always appears initially, which Hirata called an initial crack. It seems, however, that there have been few quantitative studies and little conclusive explanation for such interesting phenomena.

From the viewpoints of dynamical systems, fracture phenomena introduce a novel class of dynamical systems. Growing cracks are considered to be parts of boundary in a fracture dynamics, and therefore we can say that frac-

ture dynamics automatically selects its boundary condition without any further external operation. So far, dynamical system with possible change of the boundary condition has not been studied extensively.

The aim of this paper is to present a semi-macroscopic model which simulates the pattern of fractures due to the quenching. We shall introduce a dynamical lattice model and solve numerically the equation of motion.

The present paper consists of the followings. In the next section, we introduce a lattice model. Some advantages of the model are discussed. In §3, we formulate the method of simulation. Results of the simulations are presented in §4. It is shown that the fracture pattern suddenly changes from a few branched one to many branched one as the initial temperature increases. And quantitative characterization of patterns and real-space renormalization are discussed. The last section is devoted to conclusion and discussions.

§2. Model

It is rather straightforward to start the fracture dynamics from the equation of stress field.^{4,5)} The equation has been applied to the studies on the growth of cracks under a constant external force, because a stress field in this case can be written down explicitly. In fact, the growth of cracks under a constant stress has been investigated by using the equilibrium condition of stress field with various boundary conditions.^{6,7)}

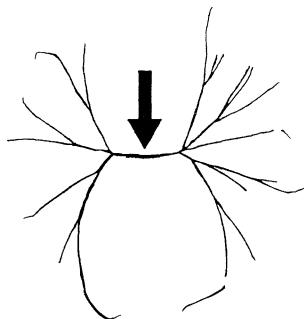


Fig. 1. A fracture pattern of a glass plate by heating. An arrow indicates an initial crack.

For the fractures caused by quenching, however, the strain changes rapidly, making the equation of stress field very complicated. Then it is sometimes difficult to use the equation of continuum. This motivates us alternatively to introduce a dynamical lattice model as an efficient description of the phenomena. In the lattice model, particles are connected to their neighboring particles by springs. The particle represents the average mass within a certain volume. Thus our model is semi-macroscopic. Since the model is not microscopic, the lattice does not have to stand for an actual crystal structure. The introduction of semi-macroscopic model is essential to an efficient simulation,⁸⁾ since a microscopic simulation is practically intractable due to the limitation of computer time.

Each spring is assumed to break down when it is stretched longer than a given threshold length. If a spring in the lattice is broken, a large strain appears around the spring. Then the neighboring springs may easily break down and cracks (i.e. a cluster of the broken springs) may grow. We numerically study the dynamics of such lattice model to investigate the evolution of cracks.

We note that the change of boundary condition by cracks is automatically included through the breakdown of springs, since we assume that the broken spring no longer has a restoring force.

The fracture by quenching is due to the stress which comes from the rapid shrink by a sudden change of temperature. To simulate this situation in our model, we reduce the natural length of springs and study the dynamics of particles after the reduction. In other words, the lattice is initially expanded and suddenly set free. A relaxation process towards a new equilibrium after the quenching is investigated. The initial expansion rate is determined by the temperature difference before and after the quenching. In this paper, we study only the case where the lattice is uniformly expanded and set free all together. This case corresponds to the uniform quenching.

For simplicity and computational efficiency, we restrict our model to a two-dimensional triangular lattice. A square lattice is not

suitable as an approximation to an isotropic continuum, because it has the directions to which no restoring force works under shear strains.

We assume that the springs obey the Hook's law below the threshold for the breakdown. For brittle materials, we believe that nonlinearity of the spring under the threshold needs not be taken into consideration.⁹⁾ Thus the dynamics of a spring is characterized by two parameters, the spring constant k , and the threshold length. Let e be elongation vector of springs connected to a particle, r position vector of the particle, m the mass of the particle and γ damping constant. The equation of motion for each particle below the threshold is expressed by

$$m \frac{d^2 r}{dt^2} = -\gamma \frac{dr}{dt} - ke. \quad (1)$$

The damping term is included since our lattice model is semi-macroscopic. The elongation vector e will be given explicitly in §3. We assume that all the springs and the particles are identical. In solving this set of equations, a small randomness is given to initial configuration of particles.

In total, we have seven parameters. The equation of motion contains four parameters; the mass m , the spring constant k , the natural length of spring (i.e. lattice spacing) a , and the damping constant γ . Three parameters in addition are the threshold of the spring, the rate of initial expansion and the randomness of initial configuration.

All of the parameters are not independent, and some of them change with the elastic constant and the scale of the material which we are interested in. Once we choose a material for simulation, the density and the elastic constant are known, then the mass of particle and the spring constant are deduced as functions of the lattice spacing. If we choose normal glass, its density is $(2.4 \sim 2.6) \times 10^3$ (kg/m³) and Young's modulus is $(7.1 \sim 8.1) \times 10^{10}$ (N/m²). From these values we can estimate $m/a^2d = (2.1 \sim 2.3) \times 10^3$ (kg/m³) and $k/d \sim O(10^{10})$ (kg/ms²). Here a is the lattice spacing and d is thickness of the material. The rate of initial expansion is deduced from the temperature difference and the thermal expansion

coefficient of the material. The threshold of the spring is chosen by an estimation of macro tensile strength of the material. It depends on the scale on which our model is thought. The randomness of initial configuration is taken to be 1%~10% of the threshold. The randomness in our model is in charge of micro cracks, impurities and density fluctuation in real materials. It is not easy to be estimated, but we believe that the assumption is not very far from reality.

The damping constant is not easily estimated, either. It is a free parameter in our model. In the present paper, we focus on the case with a large damping. A small damping case seems to lead to a different class of fractures, which will be reported in a separate paper.

§3. Method of Simulation

In a two-dimensional triangular lattice, we label a lattice site $[i, j]$ (Fig. 2). We call a particle on a site $[i, j]$ a particle $[i, j]$. This labelling is also used when particles (equivalently, sites) are in motion. A direction from $[i, j]$ to $[i+1, j]$ is referred to as a direction 1. Similarly, directions from $[i, j]$ to $[i, j+1]$ and from $[i, j]$ to $[i+1, j+1]$ are respectively referred to as direction 2 and 3. A position of particle $[i, j]$ is denoted by $r_{[i,j]}$, while the length of spring from $[i, j]$ in the direction d is written as $Rd_{[i,j]}$, $d=1, 2, 3$:

$$\begin{aligned} R1_{[i,j]} &= |r_{[i+1,j]} - r_{[i,j]}|, \\ R2_{[i,j]} &= |r_{[i,j+1]} - r_{[i,j]}|, \\ R3_{[i,j]} &= |r_{[i+1,j+1]} - r_{[i,j]}|. \end{aligned} \quad (2)$$

The equation of motion for particle $[i, j]$ below the threshold is

$$\begin{aligned} p_{[i,j]}(t+\Delta t) &= Ap_{[i,j]}(t) + B \{ (R1_{[i,j]} - a)(r_{[i+1,j]} - r_{[i,j]})/R1_{[i,j]} \\ &\quad + (R1_{[i-1,j]} - a)(r_{[i-1,j]} - r_{[i,j]})/R1_{[i-1,j]} + (R2_{[i,j]} - a)(r_{[i,j+1]} - r_{[i,j]})/R2_{[i,j]} \\ &\quad + (R2_{[i,j-1]} - a)(r_{[i,j-1]} - r_{[i,j]})/R2_{[i,j-1]} + (R3_{[i,j]} - a)(r_{[i+1,j+1]} - r_{[i,j]})/R3_{[i,j]} \\ &\quad + (R3_{[i-1,j-1]} - a)(r_{[i-1,j-1]} - r_{[i,j]})/R3_{[i-1,j-1]} \}, \end{aligned} \quad (6)$$

$$r_{[i,j]}(t+\Delta t) = r_{[i,j]}(t) + p_{[i,j]}(t+\Delta t), \quad (7)$$

where a is a natural length of spring.

In eq. (6), the variables whose time

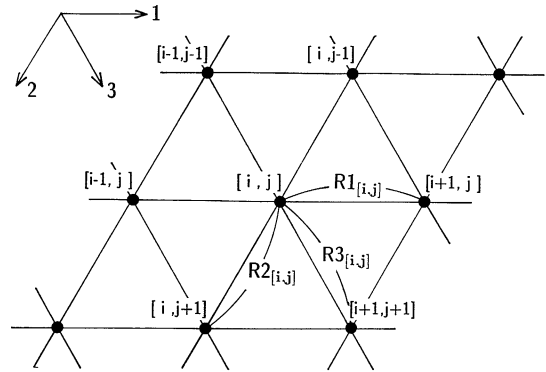


Fig. 2. Triangular lattice: site $[i, j]$ and lengths $R1_{[i,j]}$, $R2_{[i,j]}$ and $R3_{[i,j]}$. Remark that sites are not fixed in space when particles are in motion.

$$\frac{dr_{[i,j]}}{dt} = \frac{p_{[i,j]}}{m}, \quad (3)$$

$$\frac{dp_{[i,j]}}{dt} = -\frac{\gamma}{m} p_{[i,j]} - ke. \quad (4)$$

Here p is a canonical momentum to r , and e is the elongation vector of a spring. This equation is only a rewritten form of eq. (1).

We change eqs. (3) and (4) into difference equations,

$$p_{[i,j]}(t+\Delta t) = \left(1 - \Delta t \frac{\gamma}{m}\right) p_{[i,j]}(t) - \Delta t ke, \quad (5a)$$

$$r_{[i,j]}(t+\Delta t) = r_{[i,j]}(t) + \frac{\Delta t}{m} p_{[i,j]}(t+\Delta t), \quad (5b)$$

where Δt is a time interval. This difference equation is chosen so that a transformation $t \rightarrow t + \Delta t$ is symplectic when $\gamma=0$.

For simplicity we rewrite $(\Delta t/m)p$ for p , $1 - \Delta t\gamma/m$ for A and $(\Delta t)^2 k/m$ for B . Substituting a concrete expression for e , we obtain the equation of motion:

dependences are not explicitly shown are values at t . When $Rd_{[i,j]}$ is larger than the

threshold length a_{thr} for any $[i', j']$, then the corresponding term in eq. (6) should be replaced by 0 after that time. Equations (6) and (7) with this breakdown rule constitute our model of fracture.

As an initial condition, the lattice is stretched almost homogeneously with some randomness for the initial positions of particles. In addition, a definite crack is given (i.e. some springs are initially broken). We assume the free boundary condition. Lattice size is chosen to be 100×100 .

There are now five parameters in total; A and B in eqs. (6) and (7), and in addition, initial length a_0 of springs, threshold a_{thr} for the breakdown, and the average f of randomness of initial positions.

Under these conditions and with fixed values of parameters, we calculate eqs. (6) and (7) numerically and examine when and where the springs undergo breakdown. The simulation is continued until no springs will be broken any more.

§4. Results

a) Patterns of fracture

We are particularly interested in the relation between pattern of fracture and initial expansion rate, $a_0/a \equiv I$. Other parameters are fixed in the present paper. Figure 3(a)~3(d) show the final fracture patterns for various I 's. Twelve springs near the center are initially broken as marked by a thick line with an arrow.

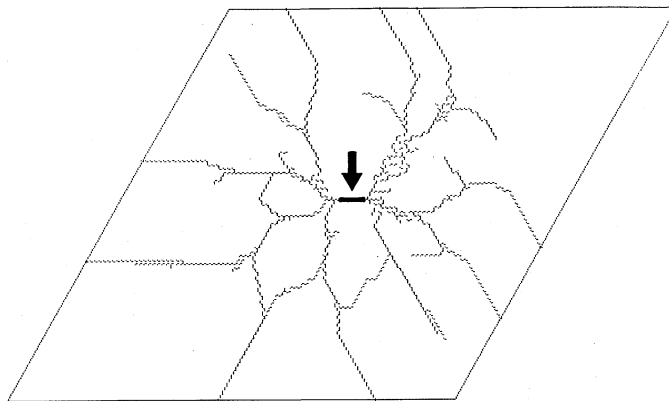
Fracture patterns in these figures consist of line segments. Each line is on the perpendicular bisector (of equilibrium positions) of broken springs, and it is drawn between centers of adjoining triangles. For example, the fracture pattern corresponding to the broken springs in Fig. 4(a) is given by Fig. 4(b). Thus the broken lines are located on a honeycomb lattice which is dual to the original triangular lattice. This seems to be the most natural way to illustrate fracture patterns of our lattice.

The fracture pattern becomes complicated with the increase of I . For small I , the fracture pattern consists of almost straight lines with a few branchings. With the increase of I , the pattern starts to have more branches. Roughly speaking, the pattern changes from tree-like to net-like.

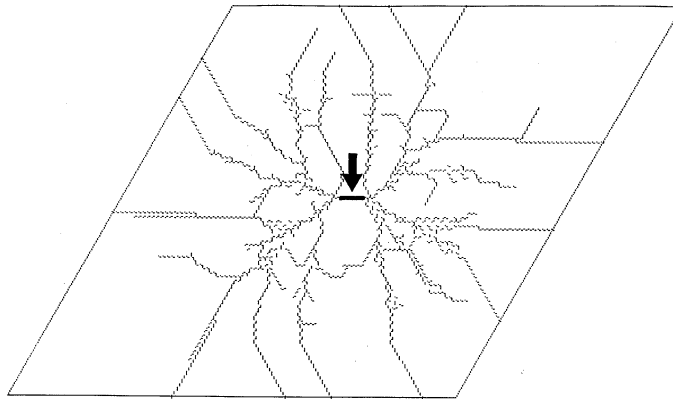
It is interesting to observe that, especially for small I , the fracture pattern near the boundary is different from the one in the bulk. This difference is attributed to the free boundary condition.

b) Number of broken springs

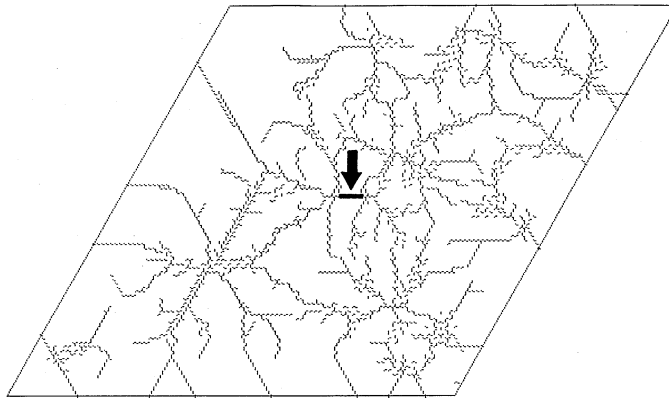
Figure 5 shows the relation between number of broken springs and initial expansion rate I . The number increases with the expansion rate I , as is expected. The increasing rate clearly changes around $I=1.0085$. Above 1.0085, the increasing rate is larger than that of below 1.0085. This can be explained as follows. Below $I=1.0085$, a crack cannot grow if a



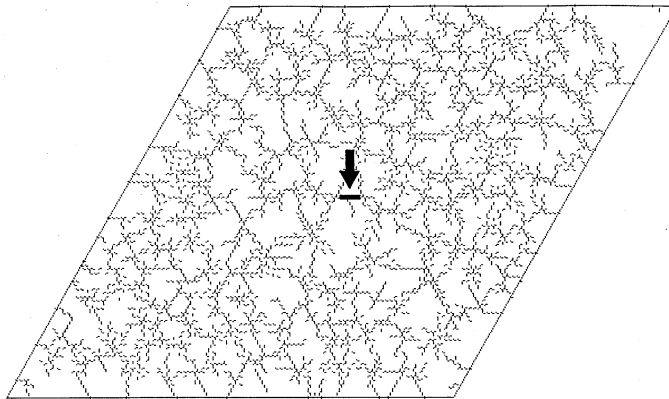
(a)



(b)

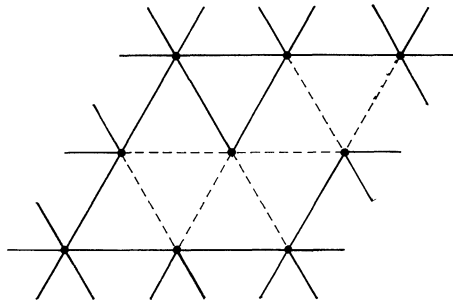


(c)

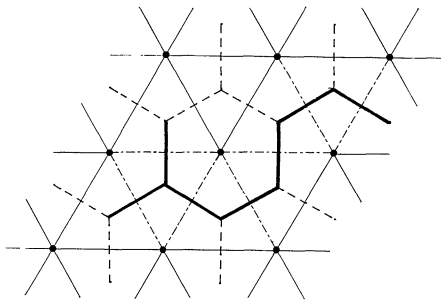


(d)

Fig. 3. Patterns of fracture. An arrow indicates a crack given initially. Parameters A , B , a_{thr} and f are fixed as $A=0.7$, $B=0.1$, $a_{\text{thr}}=1.01$ and $f=7.1 \times 10^{-4}$ (a) $I=1.0080$, (b) $I=1.0083$, (c) $I=1.0086$, (d) $I=1.0089$.



(a)



(b)

Fig. 4. (a) Broken lines represent broken springs, (b) Thick lines show pattern of cracks corresponding to Fig. (a).

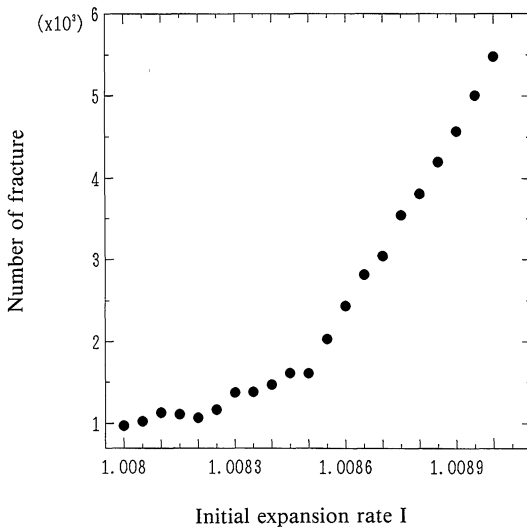


Fig. 5. Relation between initial expansion rate I and the number of broken springs.

crack is not given initially. There is no spontaneous creation of cracks. On the other hand, seeds of cracks are generated spontaneously

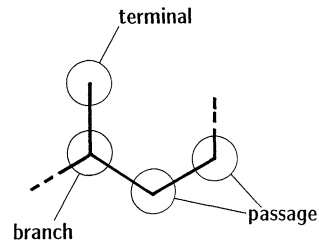


Fig. 6. Three fracture patterns for a site, terminal, passage and branch, on a dual honeycomb lattice.

for $I > 1.0085$. Thus, cracks can grow without initial crack.

We note that the number of broken springs increases linearly for $I > 1.0085$. This is not an obvious result. Indeed, the excess energy which should be released by setting the system free increases in proportional to the square of initial expansion rate I . Thus our result contradicts with a naive expectation of proportionality between the excess energy and the number of broken springs. Since the initial expansion rate measures the temperature difference before and after quenching, this result indicates that a total length of cracks increases in proportional to the temperature difference.

c) Rate of branching

As mentioned in a), we use a dual honeycomb lattice to analyze the fracture patterns. There are three links from one site of the honeycomb lattice. Thus only three kinds of fracture patterns are possible for a site (Fig. 6); *terminal* (among three links only one link is a fracture line), *passage* (two links are fracture lines), and *branch* (three links are all fracture lines). Of course, there are many sites that have *no fracture*, in addition to the above three patterns.

We have measured the number of sites belonging to each pattern for all fracture data. Figure 7 shows the relation between I and the numbers of sites of three patterns. All of the numbers of three patterns increases with I . The increasing rate changes around $I = 1.0085$. This result is consistent with the change of total number of broken springs as we mentioned in b).

To see the number of branches per unit length of cracks, we plot the ratio of the

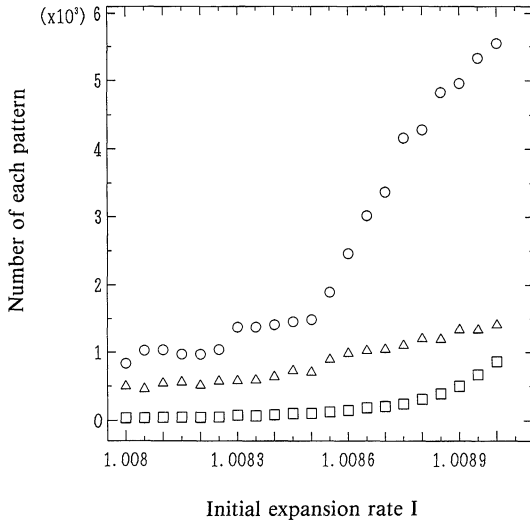


Fig. 7. Number of three fracture patterns, \circ —terminal, \triangle —passage and \square —branch, as a function of I .

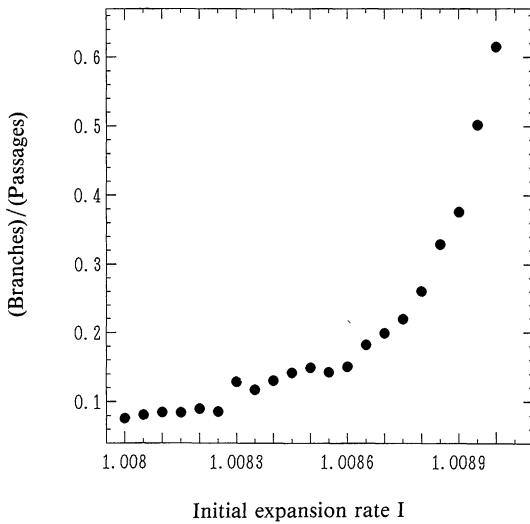


Fig. 8. Initial expansion rate I vs the rate of branches for passages.

number of branches to that of passages in Fig. 8. It shows the same tendency as Fig. 7.

d) Renormalization

To make the difference of fracture patterns more clear, we introduce the following real-space renormalization: We divide all sites of the lattice into a set of neighboring four sites. The neighboring four sites (which are con-

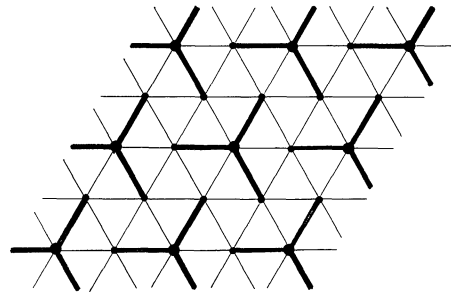


Fig. 9. A star consists of neighboring four sites which are connected by three thick lines.

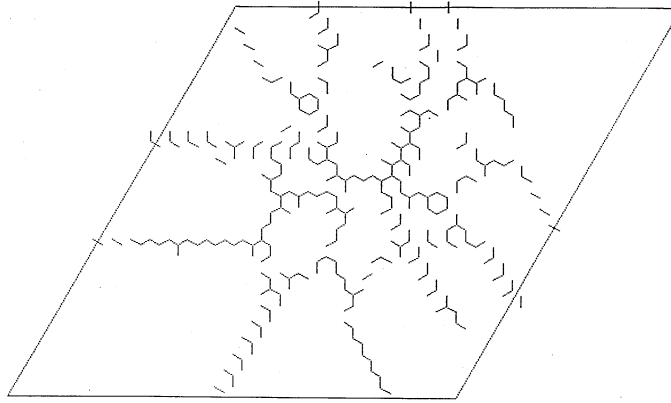
ected by three thick lines) in Fig. 9 make a *star*. There are three springs between neighboring two stars. A star is redefined as a renormalized *new* site. With this renormalization, these three springs are redefined as a *new* spring. If at least one of the three springs is broken, the *new* spring which connects the neighboring pair of *new* sites is considered to be broken.

Figures 10(a) and 10(b) show the fracture patterns after twice renormalization for Figs. 3(a) and 3(d), respectively. Size of the lattice is reduced to 25×25 from 100×100 through twice renormalization transformation. Difference between these branching patterns is emphasized compared to the original branching patterns. Figure 10(b) clearly has much larger branching rates than Fig. 10(a).

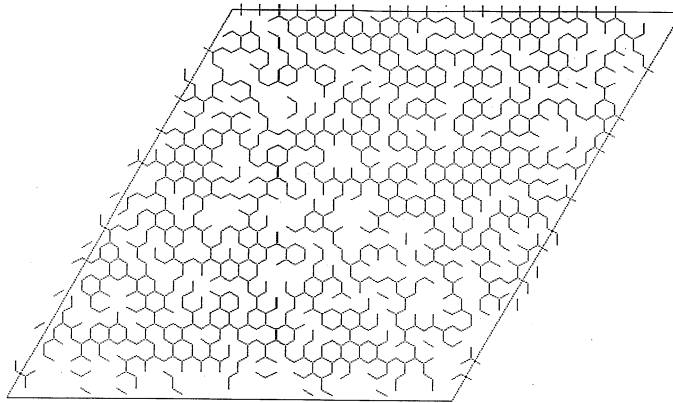
Figure 11 shows the relation between I and the numbers of three kinds of sites (i.e. terminal, passage, and branch) after we make renormalization transformation three times. Above $I=1.0085$ the rates of terminals and passages decrease, while that of branches increases. On the contrary, the rate of branches remains small even after renormalization for $I < 1.0085$.

§5. Conclusion and Discussions

In this paper, we have simulated the pattern of fractures by introducing a dynamical lattice model. This approach has some advantages over other methods. First, our model is not in a molecular scale, but in a semi-macroscopic scale. Thus the simulation of fracture does not require a large number of lattice sites. Second, it can be used even when the formulation of a strain field is very complicated. Third, we need not feedback a new boundary condition to



(a)



(b)

Fig. 10. (a) Twice renormalized pattern of Fig. 3(a), (b) Twice renormalized pattern of Fig. 3(d).

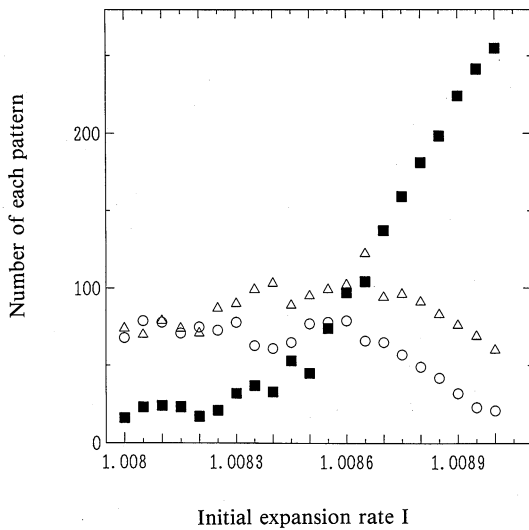


Fig. 11. Number of three fracture patterns, ○—terminal, △—passage and ■—branch, as a function of I .

solve the equation of motion in the next step.

The relation between fracture patterns and initial expansion rates has been clarified. It has been shown that fracture patterns change from a tree-like one (with a few branches) to a net-like one (with many branches) at a certain initial expansion rate, say I_c . Since the initial expansion rate measures the temperature difference before and after quenching, this result indicates that the rapid quenching causes a fracture network. That a pattern from an initial expansion rate is tree-like or net-like depends on whether seeds of crack can be generated in the initial expansion rate. Above the initial expansion rate I_c , the number of broken springs increases almost linearly.

The sudden change of fracture patterns reminds us of the transition analogous to the percolation problem. If this is the case, the properties may be analyzed by the real-space renormalization introduced in §4. Renormalization transformation brings about a flow to a fully broken state beyond the transition temperature difference, while the flow leads to a non-broken state or a single broken line from the initial crack, for a subcritical temperature difference. Although it is difficult to confirm the above statements within our small lattice, the results in §4 d) seem to suggest its validity.

Detailed quantitative experiments for the fracture by quenching are desirable. We believe that experiments will support our results, such as the sudden change of fracture patterns, the spontaneous generation of cracks for large temperature difference, and the linear increase of the total length of crack with the temperature difference.

Based on our dynamical lattice model, we may study many phenomena related to the fracture. First, the material dependence of the

pattern can be taken into account by changing other parameters, especially the initial randomness and the damping rate. Indeed, a low damping case leads to a novel class of fracture; wave-like pattern. Second, it is extremely interesting to examine whether we can reproduce various crack patterns observed experimentally by Hirata. The patterns strongly depend on the way of quenching. For example, when a glass board is successively quenched from one edge to the other, fracture patterns grows sinuously. Study on these problems is in progress and will be reported in a near future.

Acknowledgments

The authors would like to thank Dr. J. Suzuki for useful discussions. This work is partially supported by Grant-in-Aid for Scientific Research from the Ministry of Education, Science, and Culture (01540310).

References

- 1) M. Hirata: Sci. Pap. I.P.C.R. **16** (1931) No. 322, 172.
- 2) M. Hirata: RIKEN Report **8** (1929) No. 5, 52 [in Japanese].
- 3) M. Hirata: Ouyoubuturi **5** (1936) 386, 437, 482 [in Japanese].
- 4) L. D. Landau and E. M. Lifshitz: *Theory of Elasticity* (Pergamon, 1986).
- 5) A. A. Griffith: Philos. Trans. R. Soc. London, Ser. A **221** (1921) 163.
- 6) T. Kawai: Nucl. Eng. & Des. **48** (1978) 207; H. Takayasu: Prog. Theor. Phys. **74** (1985) 1343.
- 7) H. J. Herrmann: Physica D **38** (1989) 192.
- 8) The predominance of semi-macroscopic models with discrete time and space has been discussed in, K. Kaneko: in *Formation, Dynamics, and Statistics of Patterns*, ed. K. Kawasaki *et al.* (World Scientific, Singapore, 1990); A. Shinozaki and Y. Oono: Forma (1990) in press.
- 9) For the nonlinear model in one-dimensional case see for instance, M. Toda, R. Hirota and J. Satsuma: Prog. Theor. Phys. Suppl. No. 59 (1976) 148.